Bi-directional freeze casting of porous ceramics: a study of the effects of different processing parameters on microstructure

Sana Algharaibeh [a,b], Anthony J Ireland [a], Bo Su [a]*

[a] *Biomaterials Engineering Group (bioMEG), Bristol Dental School, University of Bristol, UK*

[b] *Prosthodontics Department, Faculty of Dentistry, Jordan University of Science and Technology*

*Corresponding Authors. Tel.: +44 1173429493

Email address: sana.algharaibeh@bristol.ac.uk, b.su@bristol.ac.uk

Abstract:

Highly aligned lamellar ceramic scaffolds were produced using a bi-directional freeze casting technique. A specially designed, sloped copper mould was covered with a polymer to modulate the temperature field. Effects of different processing parameters (cooling rate, mould slope angle, ceramic solid loading and binder concentration) on lamellar orientation were systematically studied. The results showed that freezing under a dual temperature gradient produced highly aligned ceramic scaffolds. Increasing both the cooling rate and the mould slope angle increased the size of the ordered ceramic region. Using different alumina solid loadings in the initial suspension had little effect on the aligned lamellar structure. Increasing the binder concentration affected ice crystal growth in a highly aligned direction. Therefore, freeze casting using a dual temperature gradient can be used to fabricate highly aligned porous materials. By controlling the microstructural features, it is possible to produce biomimetic ceramic composite materials, with potentially superior mechanical properties.

***Keywords*:** Bi-directional freeze casting; alumina; microstructure; highly aligned lamellar structure.

1. Introduction:

Freeze casting is an innovative technique that can be used to fabricate highly porous materials[1] by freezing and then removing the solvent within a ceramic suspension [2]. The technique has a number of potential advantages including: the ability to tailor the porous network by controlling the processing parameters, being applicable to a number of different materials, low tooling costs and being environmentally friendly [3]. As a result it has potential applications in a number of different fields including dentistry [4] , orthopaedics [5-7], electrical and thermal applications [8-10], filtration [11] and in wound dressings [12].

Although the freeze casting process is customisable, controlling the development of the network microstructure during processing can be challenging. Being able to reproducibly fabricate materials with a highly aligned microstructure on a large scale using freeze casting would be a great asset in materials design. Highly aligned porous materials can be of benefit for both biological [13] and industrial applications [14].

It is well documented that synthetic nacre-like materials, with a brick and mortar microstructure, can possess both high mechanical strength and toughness [15]. Launey et.al. (2009) succeeded in fabricating a nacre-like composite material from an aligned alumina scaffold infiltrated with polymethyl methacrylate (PMMA) and reported a high tensile strength of 200 MPa and a fracture toughness of 30 $MPam^{1/2}$ [16]. The same principle has been applied to hydroxyapatite/PMMA composite and the reported strength was the highest among other hydroxyapatite/PMMA composites and monolithic hydroxyapatite [17]. Bouville et.al. (2007) succeeded in fabricating a nacre-like composite based on alumina platelets and silica-calcium glasses. The material demonstrated ultrahigh strength (470 MPa) and a high fracture toughness (17.3 $MPam^{1/2}$). This nacre-like composite material was as strong as pure alumina, but with a much higher fracture toughness [18].

Several attempts have been made to control lamellar orientation during the solidifying step of freeze casting, e.g. by modifying the surface of the cooling substrates [19], or by "*freezing under flow*" [20], but both methods are complex and the results can be difficult to replicate. Another promising method, namely "bi-

directional freezing" has recently been reported, with highly aligned ceramic scaffolds up to the cm scale being fabricated [21]. Although macroscopically aligned, on a smaller microscopic scale this alignment was not always observed over the entire ceramic scaffold, and the effects of different processing parameters were also not systematically investigated. A clear understanding of how the alignment process develops within the suspension, and how different parameters affect this process, is important if the bi-directional freezing technique is to be used to produce highly aligned materials for practical applications.

In this study, bi-directional freeze casting was used to fabricate large porous ceramics with aligned lamellar microstructures using a modified mould configuration [21]. A detailed systematic investigation was carried out in order to determine how freezing under dual temperature gradient can control the nucleation and growth of ice crystals, and how different parameters may affect the final microstructure of freeze cast ceramics.

2. Materials and Methods

2.1 Materials

Alumina (Al_2O_3) powder with a particle size of 0.5 μm (CT3000SG, Almatis GmbH, Germany) was used to prepare ceramic suspensions with different solid loadings (15 to 40 vol%). In each case the alumina was mixed with distilled water and Dolapix CE64 dispersant (Zschimmer& Schwarz, Germany, 0.6 wt% of the powder weight) and after 1 hour of ball milling with yttria-stabilised zirconia balls (5 and 10 mm diameter), polyvinyl alcohol (PVA) (Sigma Aldrich, USA MW: 9,000- 10,000) at either 1,2,4 or 8wt.% of the powder weight were added to insure the green body stability after water sublimation. The whole mixture was then ball milled for a further 23 hours in order to create a colloidal system of highly dispersed alumina.

2.2 Freeze casting mould and apparatus

In conventional uni-directional freeze casting, a single flat copper base is used as one end of the temperature gradient apparatus, and vertical unidirectional crystal growth takes place from this surface. In the present experiment custom-made copper and polydimethylsiloxane (PDMS, Sylgard 184, Dow Corning, USA) wedges (60 x 60

mm) were fabricated with three different slope angles (5°, 10° and 20°). The copper wedge in each case was covered by an equivalent PDMS wedge, but upside down, to generate a horizontal temperature gradient (Fig. 1). The purpose of the two wedges, one copper and one PDMS was to provide a flat base from which to generate the ceramic sample using the freeze casting apparatus. In order to contain the ceramic slurry during this bi-directional freeze casting, an acrylic box was constructed to a height of 20mm surrounding the wedges.

Conventional freeze casting apparatus with upper and lower cooling rods were then used [22], The upper rod temperature was kept constant at 20°C throughout all the experiments using an immersion cooler (FT200, Julabo, Germany). The temperature of the bottom rod was controlled at three different cooling rates (1, 5, 10 °C/min) down to ¯30°C, again using an immersion cooler (PolyScience, Illinois, USA), but with a liquid nitrogen bath.

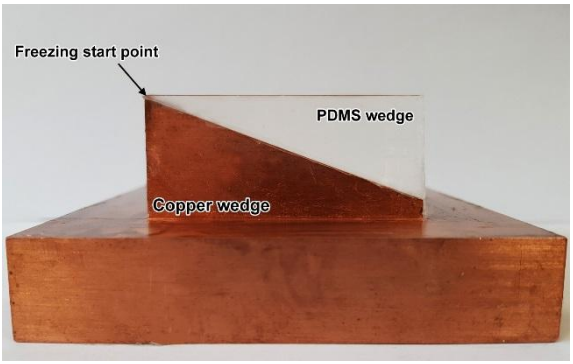

Fig. 1: Example of a copper mould (slope angle of 20°) covered by a PDMS wedge to generate bi-directional temperature gradient.

2.3 Processing and microstructure characterisation.

Following freeze casting the ice in the ceramic scaffolds was lyophilized at ¯55°C with a vacuum pressure of 0.01 mbar for 24 hours, using a freeze dryer (Modulyo, Edwards, UK). The samples were then sintered (Elite Thermal Ltd., UK) in two cycles: the first used a heating rate of 2°C/min up to 450°C, which was then held for 2 hours. The second cycle had a heating rate of 10°C/min, up to 1600°C, which was held for another 2 hours. The purpose of sintering was to burn out the binder and increase the density and strength of the green ceramic scaffolds.

The lamellar alignment and network structure of the produced scaffolds were then observed using optical (Leica DMI6000, Germany) and scanning electron microscopy (Quanta 400 - FEI Scanning Electron Microscope, USA). To improve the imaging contrast of the ceramic microstructures, the scaffolds were infiltrated with a dyed epoxy resin (Specifix, Struers, UK). To determine the axis orientation of the lamellae and the coherence, the optical images were processed using Fiji software [23]. Coherence measurements were taken every 2mm throughout the section of the scaffold along the y-axis. Interlamellar spacing and ceramic wall thickness were measured using optical microscopy (Nikon SMZ-U Zoom 1:10, Japan; and Motic Software, Motic images plus 2.0, Motic China Group Co. Ltd., China). The scaffolds were also examined using micro-CT (Nikon XTH 225 ST, UK).

3. Results

3.1 Comparison between uni-directional and bi-directional freeze casting

The effect of uni-directional versus bidirectional freeze casting on lamella alignment was performed using a slurry with a 20 vol.% ceramic loading and a 2 wt.% PVA concentration. 20 vol.% solid loading was used to study the effect of different parameters as it has previously been shown that it is possible to fabricate highly aligned ceramic scaffolds using this solid loading [21]. Fig. 2 demonstrates a schematic of conventional unidirectional freeze casting and the new bidirectional freeze casting (2a and 2d) along with both coloured stitched light microscope images (6b and 6e) and SEM images (2c and 2f). The light microscopy stitched images of the whole horizontal length of the scaffold displays different colours, each of which represent the various angles the ceramic lamellae make to the horizontal plane. Using this technique, it can be seen there is a more random nature of the lamella alignment using conventional freeze casting when compared to the bi-directional technique, which is also reflected in the SEM images of the two scaffolds. It can be seen that in the specimen fabricated using the bi-directional technique there are two distinct zones. A smaller multicoloured zone in the optical image, where the lamellae have a more random orientation, and a larger zone (visible as blue in the optical image) where the lamellae are of the same orientation. Micro-CT scan of a scaffold

prepared by bi-directional freezing was performed in order to further investigate the structure. Three dimensional models were reconstructed from the micro-CT scan. Fig. 2g is a 3D micro-CT model for the random area in the bi-directional freeze casted ceramic. It is clear that the lamellar structure is randomly aligned. The 3D micro-CT model for the aligned area of the bi-directional freeze casted ceramic (Fig. 2h) shows a highly aligned lamellar structure. Section1 of the micro CT image (Fig. 2i) shows the three typical layers seen in such freeze cast ceramics namely; dense, cellular and lamellar; with the lamellar layer being randomly aligned. The micro CT image of section 2 (Fig. 2j) shows the highly aligned lamellar structure.

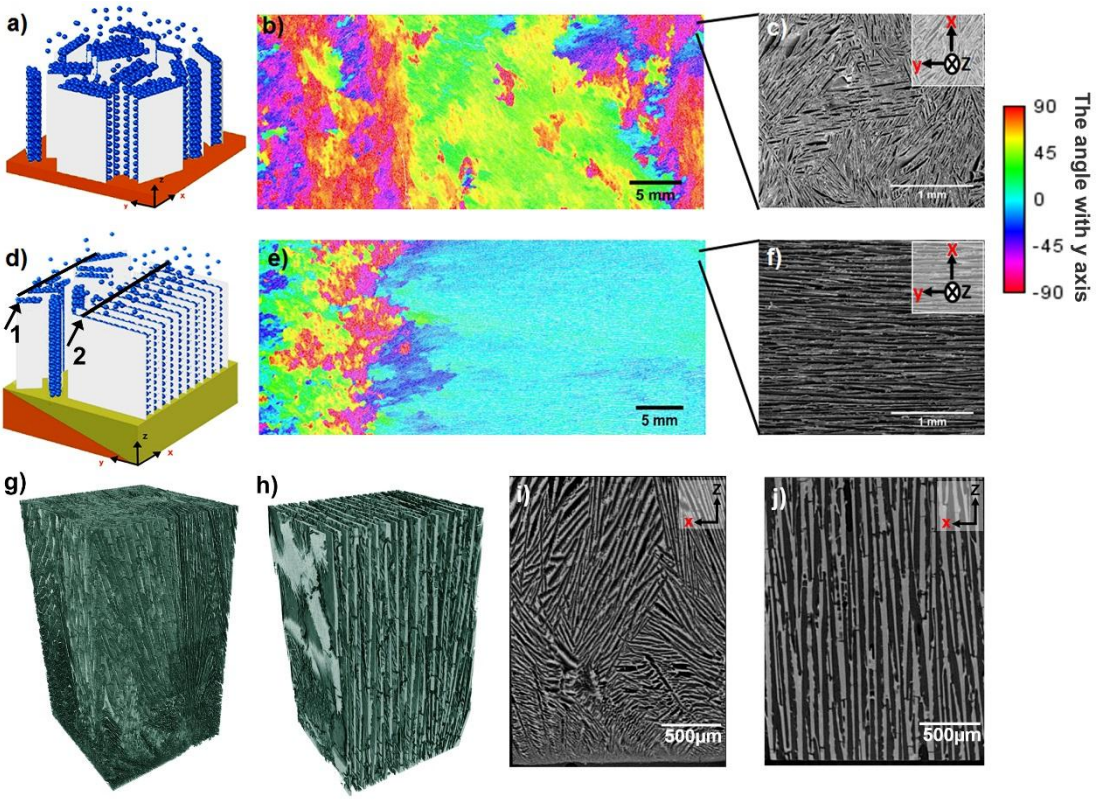

Fig. 2. Comparison of uni-directional and bi-directional freeze casting. (a) Schematic of uni-directional freeze casting, (b) coloured stitched light microscope images of random ceramic scaffold, (c) SEM image of random ceramic scaffold; (d) schematic of bi-directional freeze casting, (e) coloured stitched light microscope images of bi-directional freeze casted ceramic scaffold, (f) SEM image of the highly aligned area in the ceramic scaffold, (g) reconstructed 3D micro-CT model for the random area in bi-directional freeze casted ceramic, (h) reconstructed 3D micro-CT model for the aligned area in bi-directional freeze casted ceramic, (i) Micro-CT scan image of section 1 in (d), (j) Micro-CT scan image of section 2 in (d). The colour represents

different angles of lamellar alignment. Scaffolds were prepared from 20 vol.% alumina slurries and 2 wt.% PVA. (Freezing conditions: top temperature $^{+}$20°C, bottom temperature $^{-}$30°C, cooling rate 10°C/min).

3.2 Effects of cooling rate and mould slope angle on lamellar alignment

Since freeze casting technique is a physical process, that is highly affected by the temperature parameters such as cooling rate [24], a series of experiments were performed at different cooling rates using copper moulds with different slope angles. Once again, a ceramic solid loading of 20 vol.% and a 2 wt.% PVA concentration was used in all cases.

It can be seen from the optical images in Fig. 3 that the alignment of the lamellar structure differs significantly according to the cooling rate and the mould slope angle. An increase in cooling rate from 1 to 10°C/min, at a fixed slope angle of α = 5°, 10° or 20° increases the size of the aligned lamellar area, and the uniformity of the lamellar alignment. Likewise, with a fixed cooling rate of 1 or 5°C/min and increasing the slope angle from α = 5° to 20°. While for a cooling rate of 10°C/min a slope angle of α =20° (Fig. 3l) produces a scaffold with a larger size aligned area, but with less uniformity in alignment compared to a slope angle of α =10°, (Fig. 3k). For α =0° (flat copper base) no lamellar alignment was observed, regardless of the cooling rate. Therefore, the use of a higher cooling rate and larger slope angle appears to increase the size and the uniformity of the area of lamellar alignment.

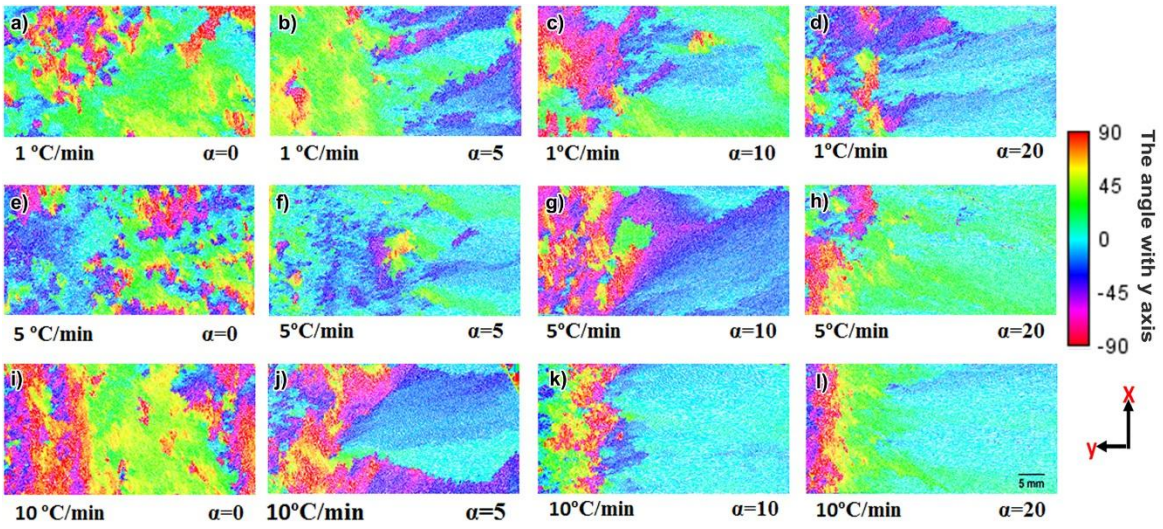

Fig. 3. Light microscope images (a-l) show the alignment of lamellar structure of ceramic samples produced at different cooling rates (1, 5 and 10 °C/min) and using copper moulds with different slope angles (α =0°, 5°, 10° and 20°). The colour

gradient represents different angles of lamellar alignment. Scaffolds were prepared from 20 vol.% alumina slurries and 2 wt.% PVA concentration. (Freezing conditions: top temperature +20°C, bottom temperature -30°C).

The measurements of the coherency in alignment of the ceramic lamellae for ceramic scaffolds prepared using the same mould slope angle (α =10°), but different cooling rates, are shown in Fig. 4. The coherency measurements were low at the initial frozen part of the scaffold (random lamellar area), but after 14-16 mm the coherency measurements began to increase, indicating a highly aligned lamellar structure in the final frozen part of the scaffold (aligned lamellar area). With increasing cooling rate, the size of the aligned lamellar area increased, as did the coherency in alignment, which reached 90% at a cooling rate of 10°C/min.

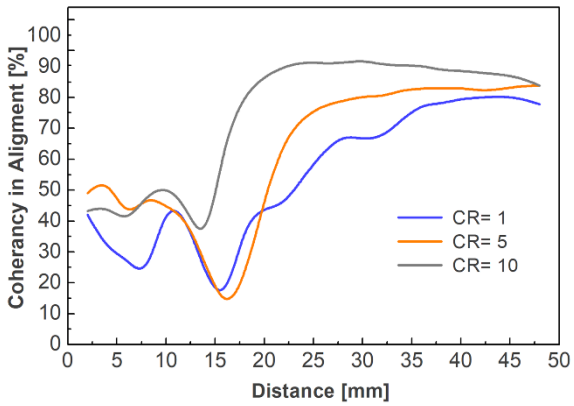

Fig. 4. Coherency in alignment of the ceramic lamellae of ceramic scaffolds as a function of cooling rate (CR). (Freezing conditions: top temperature $^{+}$20°C, bottom temperature $^{-}$30°C, mould slope angle α =10°, cooling rates: 1, 5 and 10°C/min).

The measurements of the coherency in alignment of the ceramic lamellae for scaffolds prepared using the same cooling rate (10°C/min), but different mould slope angles, are shown in Fig.5. A slope angle of α =20° produced the largest area of aligned lamellar, but with slightly lower coherency in alignment compared to a slope angle of α =10°. Both slope angles, α =10° and 20°, produced higher coherency measurements and a larger size of the aligned lamellar area compared to a slope angle of α =5°.

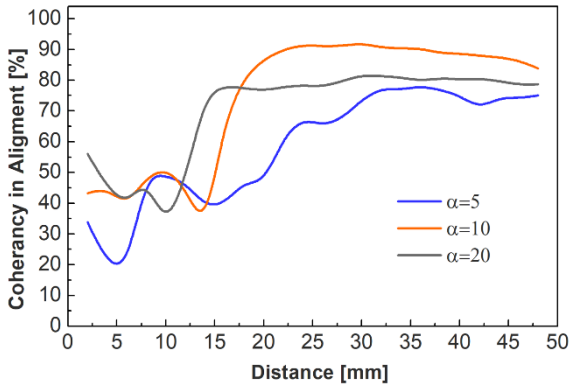

Fig. 5. Coherency in alignment of the ceramic lamellae of ceramic scaffolds as a function of slope angle. (Freezing conditions: top temperature $^{+}$20°C, bottom temperature $^{-}$30°C, cooling rates 10°C/min, mould slope angles α =5°, 10° and 20°).

3.3 Effects of cooling rate and mould slope angle on interlamellar spacing

The interlamellar spacing was measured on both the top and bottom surfaces for scaffolds prepared using the same cooling rate (CR= 10°C/min), but different mould slope angles (α = 5°, 10° and 20°) (Fig. 6). The measurements were taken from the last 5 mm of the aligned lamellar area of the scaffolds.

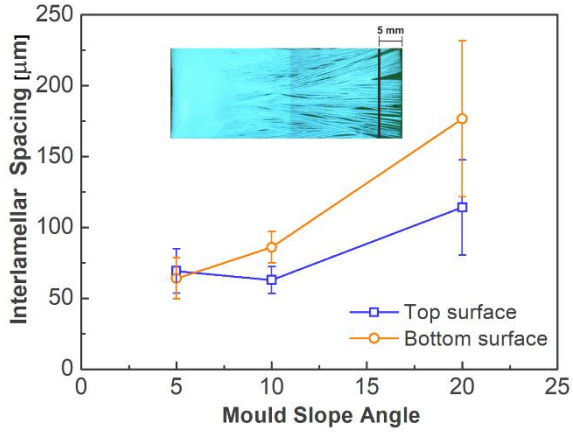

Fig. 6. Interlamellar spacing measurements for the top and bottom surfaces of ceramic scaffolds prepared using a cooling rate of 10°C/min and different mould slope angles (α = 5°, 10° and 20°). Inner image is a stitched light microscope image of the bottom side of a ceramic scaffold prepared using a cooling rate of 10°C/min and mould slope angle of 20°.

As shown in Fig. 6, a scaffold prepared with a higher slope angle (α = 20°) has a more graded pore structure, while the one prepared with a lower slope angle (α = 5°) has a more homogeneous pore structure, but with an aligned lamellar zone that is much shorter.

The bottom side of a sintered ceramic scaffold, that is in contact with polymer wedge, consists of two areas: a dense area and an aligned lamellar area. The extent of the dense area at the bottom of scaffolds prepared using different cooling rates: 1, 5 and 10°C/min, and different mould slope angles (α = 5°, 10° and 20°), were measured and are illustrated in Fig. 7. This shows that an increase in both cooling rate and mould slope angle decreases the extent of the dense area.

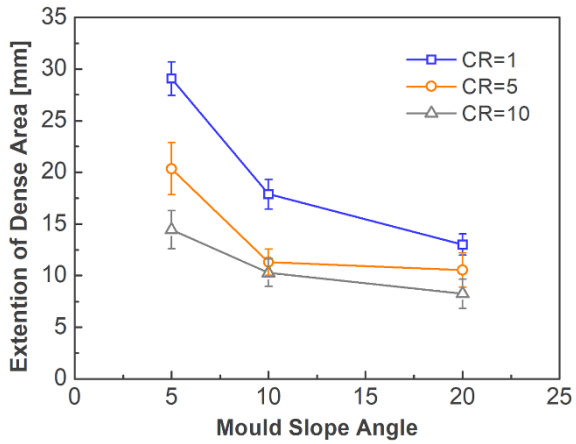

Fig. 7. Dense area measurements for ceramic scaffolds prepared using different cooling rates: 1, 5 and 10°C/min and different mould slope angles (α = 5°, 10° and 20°).

3.4 Effects of solid loading on lamellar alignment and interlamellar spacing

In the process of freeze casting the water within the ceramic slurry turns to ice that is later lyophilised to form the porous structure of the ceramic scaffold. Increasing the solid loading of the slurry means there is less water available for freezing, which in turn might affect the final scaffold microstructure and in particular the lamellar alignment. In order to investigate this, different solid loadings (10 to 40 vol.%) were tested in bi-directional freeze casting. Although using a 10 vol.% solid loading produced a very weak green ceramic that collapsed on removal from the mould, it

was possible to produce highly aligned ceramic scaffolds using different ceramic loadings up to 40 vol.% (Fig. 8).

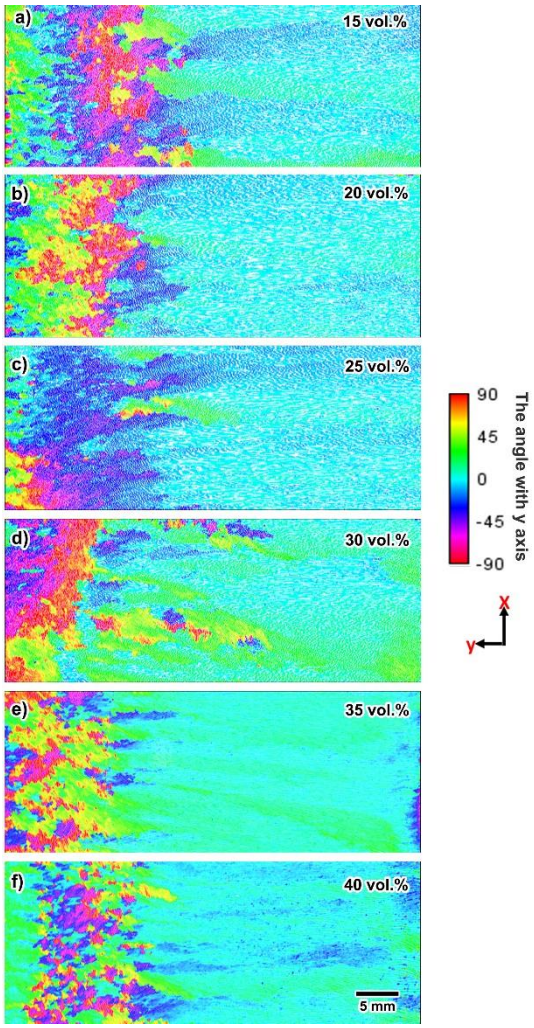

Fig. 8. Coloured stitched light microscope images of ceramic scaffolds prepared with different solid loadings, (a) 15 vol.%, (b) 20 vol.%, (c) 25 vol.%, (d) 30 vol.%, (e) 35 vol.% and (f) 40 vol.%. (Freezing conditions: top temperature +20°C, bottom temperature - 30°C, cooling rate 10°C/min, mould slope angle (α =10°), PVA concentration: 2 wt.%).

The interlamellar spacing and the ceramic wall thickness measurements were taken from the last 5 mm of the aligned lamellar area, on the top surface of the scaffolds prepared using the different solid loadings (Fig. 9).

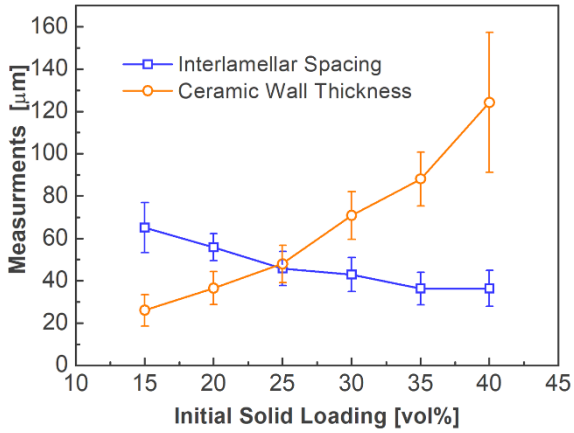

Fig. 9. Interlamellar spacing and ceramic wall thickness (µm) as a function of solid loading. (Freezing conditions: top temperature +20°C, bottom temperature: -30°C, cooling rate: 10°C/min, mould slope angle α =10°, PVA concentration: 2 wt.%).

The interlamellar spacing decreased from 65.1µm to 36.4µm when the solid loading increased from 15 vol% to 40 vol%. At the same time the ceramic wall thickness increased dramatically from 26.0µm to 124.1µm. Therefore, it would seem that using higher solid loadings in slurry preparation produces scaffolds with thicker ceramic walls and smaller interlamellar spacing.

3.5 Effects of binder concentration on lamellar alignment and interlamellar spacing

Polyvinyl alcohol (PVA) as a binder was tested at four different concentrations (1, 2, 4 and 8%) in order to study the effect on the microstructure of the ceramic scaffolds. A 20 vol.% solid loading was used for all samples. The SEM images for ceramic scaffolds prepared with different PVA concentrations (Fig. 10) would seem to indicate that as the PVA concentration increases, the interlamellar spacing decreases and produces more bridges between the ceramic walls.

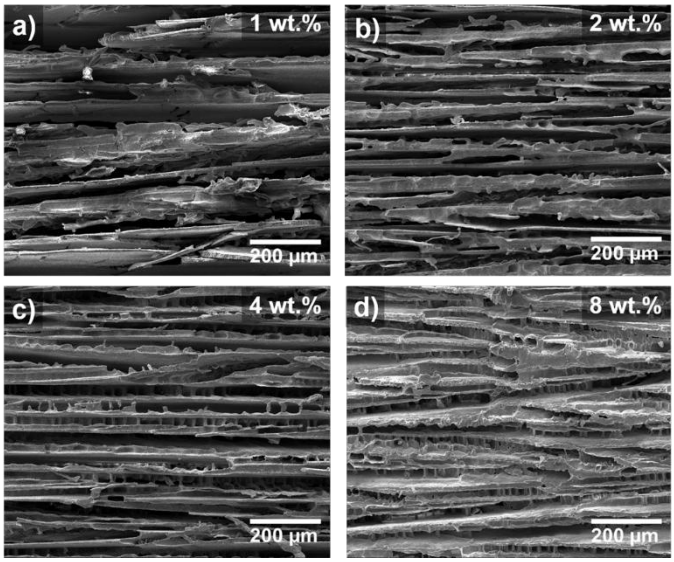

Fig. 10. SEM images for four ceramic scaffolds prepared with different PVA concentrations, (a) 1 wt.%, (b) 2 wt.%, (c) 4 wt.% and (d) 8 wt.%. (Freezing conditions: top temperature +20°C, bottom temperature -30°C, cooling rate 10°C/min, mould slope angle α= 10°, solid loading: 20 vol.%).

The interlamellar spacing and ceramic wall thickness measurements, taken from the last 5 mm of the aligned lamellar area on the top surface of the scaffolds, indicate that as the PVA concentration increases from 1 wt.% to 8 wt.%, the interlamellar spacing decreases from 82.1µm to 48.9µm, and the ceramic wall thickness increases from 35.1µm to 49.0µm (Fig. 11).

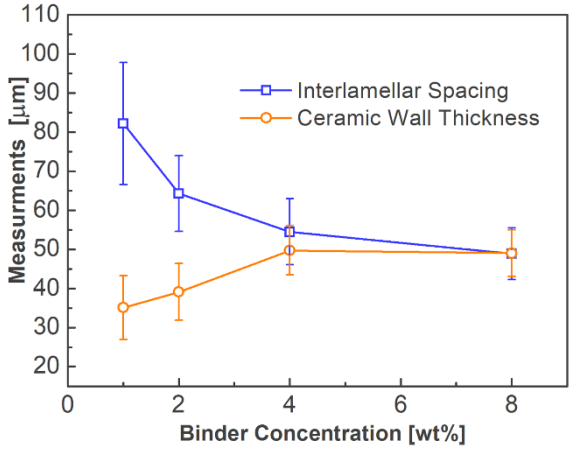

Fig. 11. Interlamellar spacing and ceramic wall thickness (μm) as a function of PVA binder concentration. (Freezing conditions: top temperature $^{+}$20°C, bottom temperature $^{-}$30°C, cooling rate 10°C/min, mould slope angle α= 10°, solid loading: 20 vol.%).

In addition, the alignment of the lamellae becomes less uniform with increasing PVA concentrations. A PVA concentration of 1% or 2wt.% does not appear to affect the alignment, whereas at the higher PVA concentrations of 4% and 8 wt.% alignment is less uniform (Fig.12).

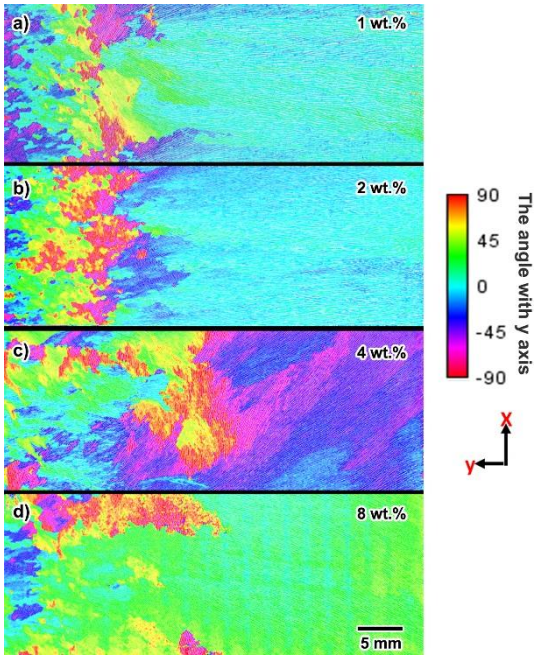

Fig. 12. Coloured stitched light microscope images of ceramic scaffolds prepared with different PVA concentration, (a) 1 wt.%, (b) 2 wt.%, (c) 4 wt.% and (d) 8 wt.%.

(Freezing conditions: top temperature +20°C, bottom temperature -30°C, cooling rate 10°C/min, mould slope angle α= 10°, solid loading: 20 vol.%).

4. Discussion

In this study we designed a novel sloped copper mould that was covered by an isolating polymer material (PDMS) to introduce a second horizontal temperature gradient during freeze casting. By using this mould, regular square shaped highly aligned ceramic scaffolds could be fabricated.

In conventional uni-directional freeze casting, where a flat copper mould is normally used, a single vertical temperature gradient develops upon freezing. Under this condition, ice crystals are allowed to nucleate and grow in a random direction, whereas in bi-directional freeze casting, the freezing occurs under the influence of dual temperature gradients determined by the mould slope angle.

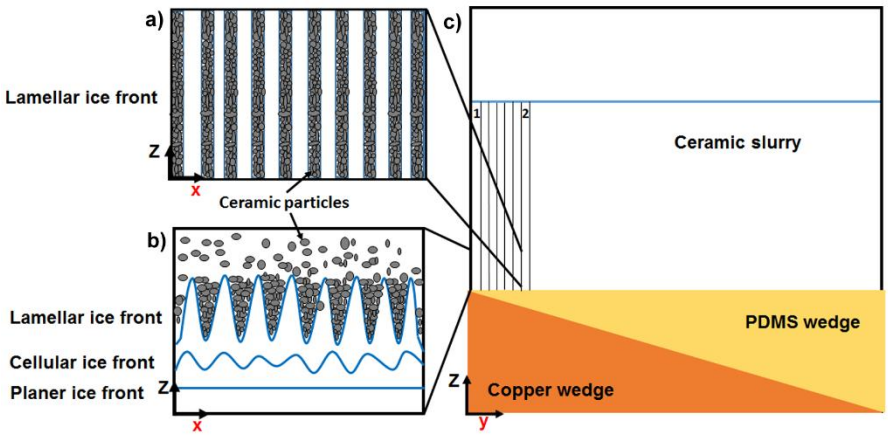

Fig. 13. Schematic diagram of a) growing lamellar ice front, b) transition of the ice front, c) the copper mould covered by PDMS wedge and the ceramic slurry inside.

At the beginning of the freezing process in the case of bi-directional freeze casting, the slurry is separated from the copper base by the thinnest part of the PDMS wedge at section 1 (Fig.13c). The first step in freezing is the formation of planar ice front which traps the ceramic particles and produces the typical dense layer at the bottom of the sample. Subsequently, the planar ice front transforms to cellular and then to lamellar crystals, and once these ice crystals start to grow they repel the ceramic

particles that have accumulated between them (Fig. 13b) [25]. The transition from the planar to lamellar ice front forces the ice crystals to nucleate in a random way, which forms the random lamellar area seen in the ceramic scaffold. These ice crystals then start to grow both vertically and horizontally. The time needed for this transition depends on the cooling rate and the higher the cooling rate the faster the transition. During this time, the same freezing process begins in the subsequent sections of the slurry. When a steady state is reached, in which the ice crystals grow under the effect of dual temperature gradient, ordered and continuous lamellar ice crystal growth is maintained throughout the slurry (Fig.13a) and no further random ice crystal nucleation occurs [26]. This process results in an ordered and highly aligned lamellar area in the ceramic scaffold. This was confirmed by the micro-CT scan (Fig. 2). The micro-CT image at section 1 (Fig. 2i) shows the three typical layers of conventional freeze cast ceramics: dense, cellular and lamellar. The lamellar layer is randomly aligned as it is the negative replica of the random ice crystals nucleation and growth. The micro-CT image in section 2 (Fig. 2j) shows a highly aligned lamellar structure, resulting from aligned ice crystal growth under the influence of the dual temperature gradient.

Based on the above analysis, two conditions should be fulfilled in ordered to increase the size of the aligned lamellar area:

1. A rapid transition of a planar to a lamellar ice front in order to produce nucleated ice crystals that are ready to grow.
2. Postponing the freezing process in the following sections as much as possible in order to give more time for water in the first sections to nucleate and produce ice crystals.

The first condition can be fulfilled by having a high cooling rate, while the second can be fulfilled by increasing the mould slope angle. This was observed in the current experiment (Fig. 3) and is in agreement with the findings of Bai et.al. (2016), who reported cooling rate and wedge angle to be the principal factors in determining the domain of lamellar alignment orientations [21]. Also, by increasing both the cooling rate and the mould slope angle the extent of the dense area at the bottom of the scaffold decreased (Fig. 7). This means that the usual process of freeze casting (having a planar ice front) is restricted to this area and once the slurry contains nucleated ice crystals that are ready to grow under the dual temperature gradient, no

further planer ice front formation takes place, it is just a process of ice crystal growth. The direction of lamellar crystal growth is parallel to the temperature gradient, as the growth of ice crystals with a crystallographic c-axis perpendicular to the temperature gradient is more favourable [26].

The scaffold prepared using a mould slope angle of α=20° showed lower coherency in alignment (Fig. 5) and a more graded structure (Fig. 6) compared to a mould slope angle of α=10°. Using a mould with a higher slope angle means that the slurry will freeze under a higher temperature gradient and will take more time to completely solidify. Under these two conditions (higher temperature gradient and longer freezing time), ice crystals will grow increasingly larger in a graded fashion to produce an inhomogeneous pore structure (Fig. 6, inner image)[27].The different sizes that ice crystals can grow to, results in a larger variation of the measurements obtained from the scaffold prepared using a mould slope angle of α=20° (Fig 6).

Ceramic solid loading has been reported as a significant parameter in controlling the microstructure of freeze cast samples [25]. In bi-directional freeze casting, water in the slurry solidifies to form ice crystals that start to grow both horizontally and vertically under the dual temperature gradient, repelling ceramic particles away from their aligned growing direction. A slurry with a high solid loading possesses less water, but this does not affect the ability of the ice crystals to grow in a highly aligned fashion, repelling the well suspended and freely moving ceramic particles. However, a higher solid loading produces scaffolds with lower interlamellar spacing and higher ceramic wall thickness (Fig. 9). The interlamellar spacing in the ceramic scaffold represent the space previously occupied by the ice crystals. Therefore increasing the solid loading increases the viscosity and reduces the amount of water, which hinders ice crystal growth in the c-axis, leading to a lower interlamellar spacing and higher ceramic wall thickness [25].

Additives such as PVA affects mainly the pore morphology of the ceramic scaffold [28]. The results showed that PVA concentration has a major influence on interlamellar spacing, ceramic wall thickness, porous network structure and lamellar alignment. When a ceramic slurry containing PVA binder freezes it goes through two stages. Before the slurry reaches 0°C, the PVA starts to gel and cover the alumina particles, producing a particle-PVA gel network. Meanwhile, the water is still in the

liquid state. As the temperature decreases further, the second stage starts. Here ice crystals nucleate and grow, with their growth restricted by the previously formed particle-PVA gel network [29]. When PVA is used at a lower concentration, the gel network is not sufficiently strong to restrict ice crystal growth, and as a result the ice crystals will grow in a more aligned direction and become larger in size, producing scaffolds with higher interlamellar spacing and lower ceramic wall thickness (Fig. 11). Increasing the PVA concentration to 4 and 8 wt.% produces a stronger interconnected gel network with an increased viscosity, that leads to an obvious change in pore morphology, more trans-lamellar ceramic bridges (Fig. 10 c and d), and deflection of ice crystals from their preferable aligned growth direction (Fig. 12).

5. Conclusions

In this study we systematically investigated the effects of various processing parameters (cooling rate, mould slope angle, solid loading and binder concentration) on bi-directional freezing and the microstructure of the resulting ceramic scaffolds. Increasing both the cooling rate and mould slope angle increased the size and uniformity of the aligned lamellar area. Using a mould slope angle of α=20° produced scaffolds with a more graded structure. Increasing the solid loading did not affect ice crystal and therefore ceramic alignment, but increasing the amount of PVA binder to 4 and 8 wt. % deflected ice crystals from their highly aligned direction of growth.

The freeze casting technique under dual temperature gradients can be used as a viable method to fabricate highly aligned porous materials. By controlling the microstructural features, it should be possible to produce nacre-like biomimetic materials with potentially superior mechanical properties.

Acknowledgments

The authors wish to thank Jordan University of Science and Technology for financial support, Wolfson Bioimaging Facility and the Elizabeth Blackwell Institute, through its Wellcome Trust ISSF Award. A special thanks to Dr. Qiang Liu, for helpful advice and discussion.

References

[1] M. Fukushima, Y.-i. Yoshizawa, T. Ohji, Macroporous Ceramics by Gelation-Freezing Route Using Gelatin, Advanced Engineering Materials 16(6) (2014) 607-620.

[2] U.G.K. Wegst, M. Schecter, A.E. Donius, P.M. Hunger, Biomaterials by freeze casting, Philosophical Transactions of the Royal Society a-Mathematical Physical and Engineering Sciences 368(1917) (2010) 2099-2121.

[3] R. Liu, T. Xu, C.-a. Wang, A review of fabrication strategies and applications of porous ceramics prepared by freeze-casting method, Ceramics International 42(2) (2016) 2907-2925.

[4] S. Al-Jawoosh, A. Ireland, B. Su, Fabrication and characterisation of a novel biomimetic anisotropic ceramic/polymer-infiltrated composite material, Dental Materials 34(7) (2018) 994-1002.

[5] S. Deville, E. Saiz, R.K. Nalla, A.P. Tomsia, Freezing as a path to build complex composites, Science 311(5760) (2006) 515-518.

[6] B.H. Yoon, C.S. Park, H.E. Kim, Y.H. Koh, In-situ fabrication of porous hydroxyapatite (HA) scaffolds with dense shells by freezing HA/camphene slurry, Materials Letters 62(10-11) (2008) 1700-1703.

[7] E. Babaie, S.B. Bhaduri, Fabrication Aspects of Porous Biomaterials in Orthopedic Applications: A Review, ACS Biomater. Sci. Eng. 4(1) (2018) 1-39.

[8] N. Soltani, R. Martinez-Bautista, A. Bahrami, L.H. Arcos, M. Cassir, J.C. Carvayar, Fabrication of aligned porous LaNi0.6Fe0.4O3 perovskite by water based freeze casting, Chem. Phys. Lett. 700 (2018) 138-144.

[9] S.Y. Zhu, L.H. Cao, Z.W. Xiong, C.J. Lu, Z.P. Gao, Enhanced piezoelectric properties of 3-1 type porous 0.94Bi(0.5)Na(0.5)TiO(3)-0.06BaTiO(3) ferroelectric ceramics, Journal of the European Ceramic Society 38(4) (2018) 2251-2255.

[10] X.L. Zeng, L. Ye, S.H. Yu, R. Sun, J.B. Xu, C.P. Wong, Facile Preparation of Superelastic and Ultra low Dielectric Boron Nitride Nanosheet Aerogels via Freeze-Casting Process, Chemistry of Materials 27(17) (2015) 5849-5855.

[11] Y.F. Tang, M.C. Mao, S. Qiu, K. Zhao, Fabrication of porous ceramics with double-pore structure by stepwise freeze casting using water/diphenyl methane emulsion, Ceramics International 44(1) (2018) 1187-1192.

[12] S. Feiz, A.H. Navarchian, O.M. Jazani, Poly(vinyl alcohol) membranes in wound-dressing application: microstructure, physical properties, and drug release behavior, Iran. Polym. J. 27(3) (2018) 193-205.

[13] J.R. Rodrigues, N.M. Alves, J.F. Mano, Nacre-inspired nanocomposites produced using layer-by-layer assembly: Design strategies and biomedical applications, Materials Science & Engineering C-Materials for Biological Applications 76 (2017) 1263-1273.

[14] H. Zhao, Z. Yang, L. Guo, Nacre-inspired composites with different macroscopic dimensions: strategies for improved mechanical performance and applications, NPG Asia Materials (2018).

[15] U.G.K. Wegst, H. Bai, E. Saiz, A.P. Tomsia, R.O. Ritchie, Bioinspired structural materials, Nature Materials 14(1) (2015) 23-36.

[16] M.E. Launey, E. Munch, D.H. Alsem, H.B. Barth, E. Saiz, A.P. Tomsia, R.O. Ritchie, Designing highly toughened hybrid composites through nature-inspired hierarchical complexity, Acta Materialia 57(10) (2009) 2919-2932.
[17] H. Bai, F. Walsh, B. Gludovatz, B. Delattre, C. Huang, Y. Chen, A.P. Tomsia, R.O. Ritchie, Bioinspired Hydroxyapatite/Poly(methyl methacrylate) Composite with a Nacre-Mimetic Architecture by a Bidirectional Freezing Method, Advanced Materials 28(1) (2016) 50-56.
[18] F. Bouville, E. Maire, S. Meille, B. Van de Moortele, A.J. Stevenson, S. Deville, Strong, tough and stiff bioinspired ceramics from brittle constituents (vol 13, pg 508, 2014), Nature Materials 16(12) (2017) 1271-1271.
[19] E. Munch, E. Saiz, A.P. Tomsia, S. Deville, Architectural Control of Freeze-Cast Ceramics Through Additives and Templating, Journal of the American Ceramic Society 92(7) (2009) 1534-1539.
[20] F. Bouville, E. Portuguez, Y.F. Chang, G.L. Messing, A.J. Stevenson, E. Maire, L. Courtois, S. Deville, Templated Grain Growth in Macroporous Materials, Journal of the American Ceramic Society 97(6) (2014) 1736-1742.
[21] H. Bai, Y. Chen, B. Delattre, A.P. Tomsia, R.O. Ritchie, Bioinspired large-scale aligned porous materials assembled with dual temperature gradients, Science advances 1(11) (2015) e1500849.
[22] A. Preiss, B. Su, S. Collins, D. Simpson, Tailored graded pore structure in zirconia toughened alumina ceramics using double-side cooling freeze casting, Journal of the European Ceramic Society 32(8) (2012) 1575-1583.
[23] J. Schindelin, I. Arganda-Carreras, E. Frise, V. Kaynig, M. Longair, T. Pietzsch, S. Preibisch, C. Rueden, S. Saalfeld, B. Schmid, J.Y. Tinevez, D.J. White, V. Hartenstein, K. Eliceiri, P. Tomancak, A. Cardona, Fiji: an open-source platform for biological-image analysis, Nat. Methods 9(7) (2012) 676-682.
[24] M.M. Porter, R. Imperio, M. Wen, M.A. Meyers, J. McKittrick, Bioinspired Scaffolds with Varying Pore Architectures and Mechanical Properties, Adv. Funct. Mater. 24(14) (2014) 1978-1987.
[25] S. Deville, Freeze-casting of porous ceramics: A review of current achievements and issues, Advanced Engineering Materials 10(3) (2008) 155-169.
[26] S. Deville, E. Saiz, A.P. Tomsia, Ice-templated porous alumina structures, Acta Materialia 55(6) (2007) 1965-1974.
[27] W.L. Li, K. Lu, J.Y. Walz, Freeze casting of porous materials: review of critical factors in microstructure evolution, International Materials Reviews 57(1) (2012) 37-60.
[28] K.H. Zuo, Y.P. Zeng, D.L. Jiang, Effect of cooling rate and polyvinyl alcohol on the morphology of porous hydroxyapatite ceramics, Materials & Design 31(6) (2010) 3090-3094.
[29] K.H. Zuo, Y.P. Zeng, D.L. Jiang, Effect of polyvinyl alcohol additive on the pore structure and morphology of the freeze-cast hydroxyapatite ceramics, Materials Science & Engineering C-Materials for Biological Applications 30(2) (2010) 283-287.

Figure Captions

Fig. 1: Example of a copper mould (slope angle of 20°) covered by a PDMS wedge to generate bi-directional temperature gradient.

Fig. 2. Comparison of uni-directional and bi-directional freeze casting. (a) Schematic of uni-directional freeze casting, (b) coloured stitched light microscope images of random ceramic scaffold, (c) SEM image of random ceramic scaffold; (d) schematic of bi-directional freeze casting, (e) coloured stitched light microscope images of bi-directional freeze casted ceramic scaffold, (f) SEM image of the highly aligned area in the ceramic scaffold, (g) reconstructed 3D micro-CT model for the random area in bi-directional freeze casted ceramic, (h) reconstructed 3D micro-CT model for the aligned area in bi-directional freeze casted ceramic, (i) Micro-CT scan image of section 1 in (d), (j) Micro-CT scan image of section 2 in (d). The colour represents different angles of lamellar alignment. Scaffolds were prepared from 20 vol.% alumina slurries and 2 wt.% PVA. (Freezing conditions: top temperature +20°C, bottom temperature -30°C, cooling rate 10°C/min).

Fig. 3. Light microscope images (a-l) show the alignment of lamellar structure of ceramic samples produced at different cooling rates (1, 5 and 10 °C/min) and using copper moulds with different slope angles (α =0°, 5°, 10° and 20°). The colour gradient represents different angles of lamellar alignment. Scaffolds were prepared from 20 vol.% alumina slurries and 2 wt.% PVA concentration. (Freezing conditions: top temperature +20°C, bottom temperature -30°C).

Fig. 4. Coherency in alignment of the ceramic lamellae of ceramic scaffolds as a function of cooling rate (CR). (Freezing conditions: top temperature +20°C, bottom temperature -30°C, mould slope angle α =10°, cooling rates: 1, 5 and 10°C/min).

Fig. 5. Coherency in alignment of the ceramic lamellae of ceramic scaffolds as a function of slope angle. (Freezing conditions: top temperature +20°C, bottom temperature -30°C, cooling rates 10°C/min, mould slope angles α =5°, 10° and 20°).

Fig. 6. Interlamellar spacing measurements for the top and bottom surfaces of ceramic scaffolds prepared using a cooling rate of 10°C/min and different mould slope angles (α = 5°, 10° and 20°). Inner image is a stitched light microscope image of the bottom side of a ceramic scaffold prepared using a cooling rate of 10°C/min and mould slope angle of 20°.

Fig. 7. Dense area measurements for ceramic scaffolds prepared using different cooling rates: 1, 5 and 10°C/min and different mould slope angles (α = 5°, 10° and 20°).

Fig. 8. Coloured stitched light microscope images of ceramic scaffolds prepared with different solid loadings, (a) 15 vol.%, (b) 20 vol.%, (c) 25 vol.%, (d) 30 vol.%, (e) 35 vol.% and (f) 40 vol.%. (Freezing conditions: top temperature +20°C, bottom temperature - 30°C, cooling rate 10°C/min, mould slope angle (α =10°), PVA concentration: 2 wt.%).

Fig. 9. Interlamellar spacing and ceramic wall thickness (µm) as a function of solid loading. (Freezing conditions: top temperature +20°C, bottom temperature: -30°C, cooling rate: 10°C/min, mould slope angle α =10°, PVA concentration: 2 wt.%).

Fig. 10. SEM images for four ceramic scaffolds prepared with different PVA concentrations, (a) 1 wt.%, (b) 2 wt.%, (c) 4 wt.% and (d) 8 wt.%. (Freezing conditions: top temperature +20°C, bottom temperature -30°C, cooling rate 10°C/min, mould slope angle α= 10°, solid loading: 20 vol.%).

Fig. 11. Interlamellar spacing and ceramic wall thickness (µm) as a function of PVA binder concentration. (Freezing conditions: top temperature +20°C, bottom temperature -30°C, cooling rate 10°C/min, mould slope angle α= 10°, solid loading: 20 vol.%).

Fig. 12. Coloured stitched light microscope images of ceramic scaffolds prepared with different PVA concentration, (a) 1 wt.%, (b) 2 wt.%, (c) 4 wt.% and (d) 8 wt.%. (Freezing conditions: top temperature +20°C, bottom temperature -30°C, cooling rate 10°C/min, mould slope angle α= 10°, solid loading: 20 vol.%).

Fig. 13. Schematic diagram of a) growing lamellar ice front, b) transition of the ice front, c) the copper mould covered by PDMS wedge and the ceramic slurry inside.